

Pion double charge exchange on ^{12}C at low energies

J. A. Faucett, M. W. Rawool, and K. S. Dhuga
New Mexico State University, Las Cruces, New Mexico 88003

J. D. Zumbro, R. Gilman,* and H. T. Fortune
University of Pennsylvania, Philadelphia, Pennsylvania 19104

C. L. Morris and M. A. Plum
Los Alamos National Laboratory, Los Alamos, New Mexico 87545
 (Received 6 October 1986)

An excitation function from $T_\pi=50$ to 120 MeV at $\theta_{\text{lab}}=35^\circ$ and an angular distribution at 60 MeV have been measured for the pion double-charge-exchange reaction $^{12}\text{C}(\pi^+, \pi^-)^{12}\text{O}(\text{g.s.})$. The cross section is found to decrease with increasing energy. The ^{12}C excitation function and the angular distribution are very similar in shape to those of the double-isobaric-analog-state transitions observed for ^{14}C and ^{18}O , but the magnitude is a factor of 6 smaller.

At energies above 100 MeV, the pion double-charge-exchange (DCX) reaction has been studied extensively.^{1,2} For transitions to residual double-isobaric-analog states (DIAS's), sufficient data exist that the various systematic features of the reaction (the extracted energy, angle, and mass dependences) may be considered well established. Many theoretical studies have indicated the importance of various processes for predictions of double charge exchange.³ In contrast, transitions leading to residual nonanalog ground states have not been as extensively studied theoretically, despite the large amount of data for those transitions. Experimental nonanalog cross sections² in light nuclei are typically within a factor of 2 [near the $\Delta(3,3)$ resonance] of those for DIAS transitions in nuclei of similar mass.¹ Systematic features of the data² are different from those exhibited by DIAS transitions.

Recently, there has been much interest in the DCX reaction to DIAS at low energies, because of the large cross sections observed experimentally,⁴⁻⁶ and because of the suggestion that six-quark bag effects may play a prominent role in explaining the data.⁷ However, more conventional explanations of the large cross sections have subsequently appeared. In the Δ -hole model, the large cross sections result from contributions involving nonanalog intermediate states.⁸ In multiple scattering theory, two-nucleon correlations are important and the DCX cross section at forward angles results mostly from two large-angle single-charge-exchange scatterings ($\theta_{\text{scat}} \sim 90^\circ$) from two nucleons with a relative separation of less than 1 fm.⁹

The Δ -hole-model results directly imply that some nonanalog residual states will also be strongly excited at low energies. Calculations performed within the Δ -hole model for $^{16}\text{O}(\pi^+, \pi^-)^{16}\text{N}(\text{g.s.})$ predict a forward angle cross section of about $1 \mu\text{b}/\text{sr}$.⁸ Presumably, each large angle scattering in the multiple-scattering theory leads to a large probability of nonzero angular-momentum transfer, and thus to nonanalog residual states.

To test the idea that the large cross sections are a phenomenon not unique to DIAS transitions, we have extended measurements of nonanalog DCX to lower ener-

gies. We report here the measurement of an excitation function for the non-DIAS transition $^{12}\text{C}(\pi^+, \pi^-)^{12}\text{O}(\text{g.s.})$ at 35° from 50 to 120 MeV and of an angular distribution at 60 MeV.

The experiment was performed at the low energy pion channel of the Clinton P. Anderson Meson Physics Facility (LAMPF) with the Clamshell spectrometer. The general characteristics of the spectrometer are as described in Ref. 10. The channel momentum spread ranged from 0.2% to 0.6% depending on the energy, and was determined by the need to resolve the ground state and first excited state of the residual ^{12}O nucleus. The scattering chamber was vacuum coupled to both the channel and the spectrometer. Following the scattering chamber and before the spectrometer was a 0.32 cm scintillator (S1). The spectrometer focal plane included two 0.64 cm scintillators (S2 and S3), two X-Y drift chambers,¹¹ and a thick (15.2 cm) scintillator (S4). The first three scintillators defined the event trigger (S1·S2·S3) and also provided time-of-flight (TOF) for particle identification. The X-Y drift chambers measured the position and angle in both X and Y in order to determine the momentum of each particle. The last three scintillators (S2, S3, and S4) measured the total energy. Muons and electrons were rejected by comparing this total energy with the value computed from the measured momentum, and by TOF identification. The resolution, which was limited by the channel momentum spread and the energy straggling in the target and front scintillator, was approximately 1 MeV. The solid-angle acceptance of the spectrometer was about 40 msr.

A toroidal pickup loop was used for monitoring the primary proton beam. Except for the 120-MeV data, normalization of the cross sections was accomplished by comparing yields from elastic π^+ - ^{12}C scattering with the published cross sections.¹² For the 120-MeV data, normalization factors were determined by comparing π^+ p scattering yields with cross sections calculated from phase shifts.¹³

The target was 470 mg/cm² natural graphite. A spec-

trum containing the sum of all the raw 60-MeV data is displayed in Fig. 1. The data in this figure have not been corrected for the spectrometer acceptance and no normalizations were applied to the data before summing. The reaction has a Q value of -31 MeV and the lowest excited states of ^{12}O were observed at approximately 1.3 and 2.8 MeV. The compilation by Ajzenberg-Selove¹⁴ shows only a state at about 1.0 MeV.

The measured angular distribution from 25° to 95° at 60 MeV is given in Table I. Figure 2 shows the angular distribution along with the results for the DIAS transitions in ^{14}C and ^{18}O near 50 MeV.^{5,6} The ^{12}C cross sections are a factor of 6 smaller than those of the other two nuclei but all of the shapes are similar. The measured excitation function at 35° for this experiment is given in Table II and is shown in Fig. 3. The data were taken at 35° since at more forward angles the front scintillator was unable to handle the high rates without a considerable reduction in beam intensity.

For ^{14}C and ^{18}O at low energies, the measured angular distributions have been extrapolated to zero degrees in order to compare low-energy data with data in the 100–300 MeV range.^{5,6} We have used the following technique for extrapolation of the present ^{12}C measurements to zero degrees. The 60-MeV angular distribution was fitted by the function $NJ_0^2(qR)$, where N is a normalization, q is the momentum transfer, and R is a size parameter. A similar parametrization provides a good representation of resonance energy nonanalog angular distributions.^{2,15} This fit, at 60 MeV, provides a 0° cross section of $0.50 \pm 0.08 \mu\text{b/sr}$ and yields a value of $2.31 \pm 0.16 \text{ fm}$ for R . For the other three energies (50, 80, and 100 MeV), we have assumed the angular distribution to be the same function of momentum transfer as at 60 MeV, and have fitted those data by varying only the normalization parameter N . This assumption allows the 35° excitation function to be transformed into a 0° one. (We estimate the technique to

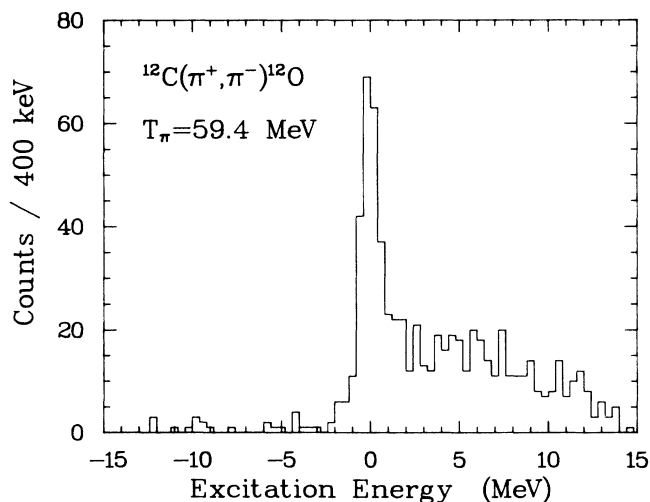


FIG. 1. Spectrum of the reaction $^{12}\text{C}(\pi^+, \pi^-)^{12}\text{O}$ at $T_\pi = 60$ MeV, containing the sum of all data ($\theta_{\text{lab}} = 25^\circ - 95^\circ$).

TABLE I. Cross sections for $^{12}\text{C}(\pi^+, \pi^-)^{12}\text{O}(\text{g.s.})$ at 59.4 MeV.

$\theta_{\text{c.m.}}$ (deg)	$d\sigma/d\Omega_{\text{c.m.}}$ ($\mu\text{b/sr}$)
25.6	0.606 ± 0.099
35.8	0.300 ± 0.077
51.0	0.336 ± 0.066
66.2	0.220 ± 0.047
81.3	0.138 ± 0.033
96.3	0.124 ± 0.023

be accurate to within about 50%.) The forward angle results are displayed in Fig. 4 (the errors bars shown include the statistical uncertainties and the uncertainty in the fitted value of R), along with ^{12}C results at higher energies and data for ^{14}C .^{2,3,16,17} Below about 150 MeV, the two excitation functions are strikingly similar in shape, differing only in magnitude. Thus, the large rise observed at 50 MeV for DIAS DCX is also present in this nonanalog transition.

The similarity in behavior of the data on ^{12}C , ^{14}C , and ^{18}O is quite striking. Cross sections for each nucleus increase by a factor of ~ 5 as incident energy decreases

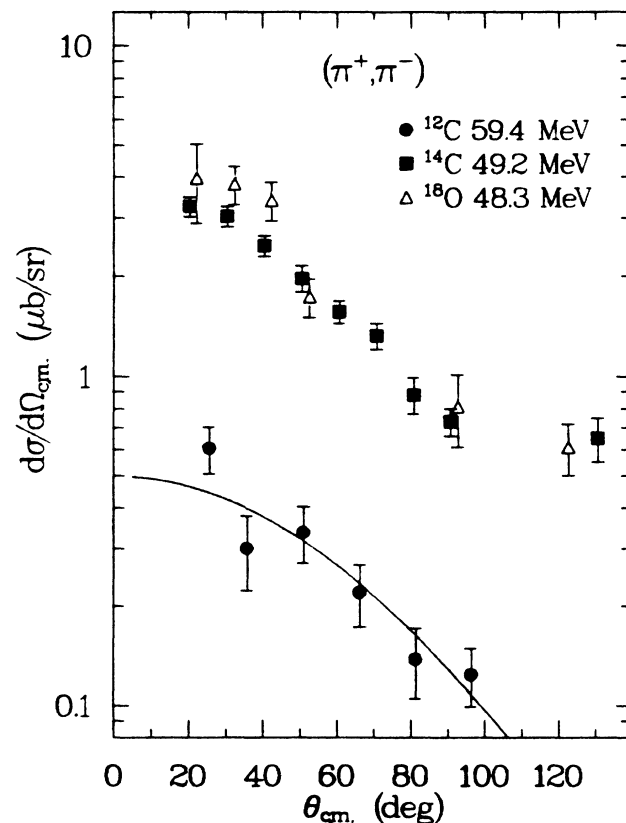


FIG. 2. DCX angular distributions on ^{12}C at 60 MeV and on ^{14}C and ^{18}O at 50 MeV. The circles are from the present work, the squares from Ref. 5, and the triangles from Ref. 6. The line is the function $NJ_0^2(qR)$ fit to the data.

TABLE II. Cross sections for $^{12}\text{C}(\pi^+, \pi^-)^{12}\text{O}(\text{g.s.})$ at $\theta_{\text{lab}} = 35^\circ$.

T_π (MeV)	$d\sigma/d\Omega_{\text{c.m.}}$ ($\mu\text{b}/\text{sr}$)
49.3	0.566 ± 0.131
59.4	0.300 ± 0.077
79.4	0.146 ± 0.019
99.5	0.072 ± 0.019
119.5	< 0.048

from 100 to 50 MeV. The angular distributions have roughly the same shape, although the nuclei have different sizes. These similarities hold even though ^{14}C and ^{18}O are DIAS transitions and ^{12}C is a nonanalog transition. Also, the kinematics are different for the ^{12}C reaction, for which the Q value is over 25 MeV more negative than that for the ^{14}C or ^{18}O reactions.

At higher energies (~ 300 MeV), DIAS DCX is believed to be dominated by transitions through the intermediate analog state, and the ratio of DIAS to nonanalog cross sections is typically 20 or larger.¹⁶ In addition, for energies between about 180 and 300 MeV, DIAS cross section rise monotonically with energy at forward angles, while nonanalog transitions decrease. At those energies, the DIAS angular distributions are diffractive. For energies below about 180 MeV, the behavior is quite different. On resonance, for example, nonanalog DCX angular distributions appear simply diffractive,¹⁵ whereas those for

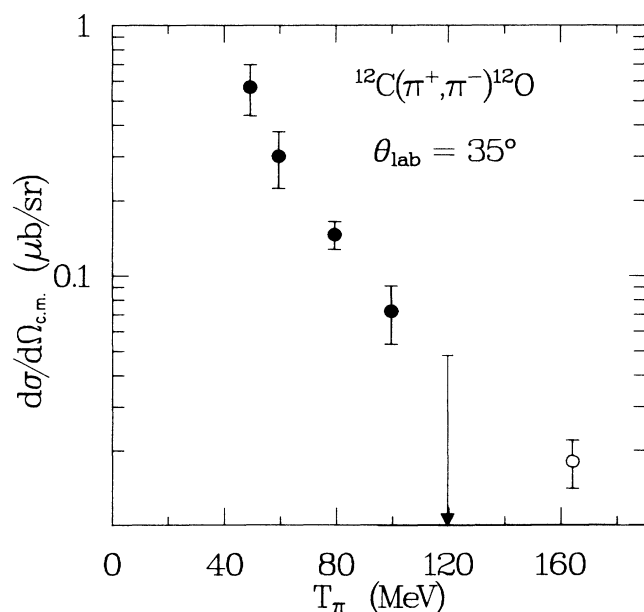


FIG. 3. DCX excitation function for ^{12}C at $\theta_{\text{lab}} = 35^\circ$. The filled circles are from the present work and the open circle is from Ref. 2.

DIAS transitions do not.¹⁸

At 50 MeV, there appears to be little selectivity for analog transitions. In light nuclei, such as ^{12}C , ^{14}C , and ^{18}O , excited states may be suppressed due both to kinematics (the reaction is closer to threshold than for the transition to the ground state) and to nuclear structure. In heavier nuclei, however, the lack of selectivity may make it difficult to observe the DIAS above a continuum background. However, the collective feature of transitions to the residual ground state may make this state strong for all targets.

In conclusion, while the present measurements cannot discriminate between six-quark, Δ -hole, and multiple-scattering explanations, they do emphasize that the phenomenon of an increasing (π^+, π^-) cross section with decreasing energy does not require the identical initial and final structure of analog states.

This work was supported in part by the U.S. Department of Energy and the National Science Foundation.

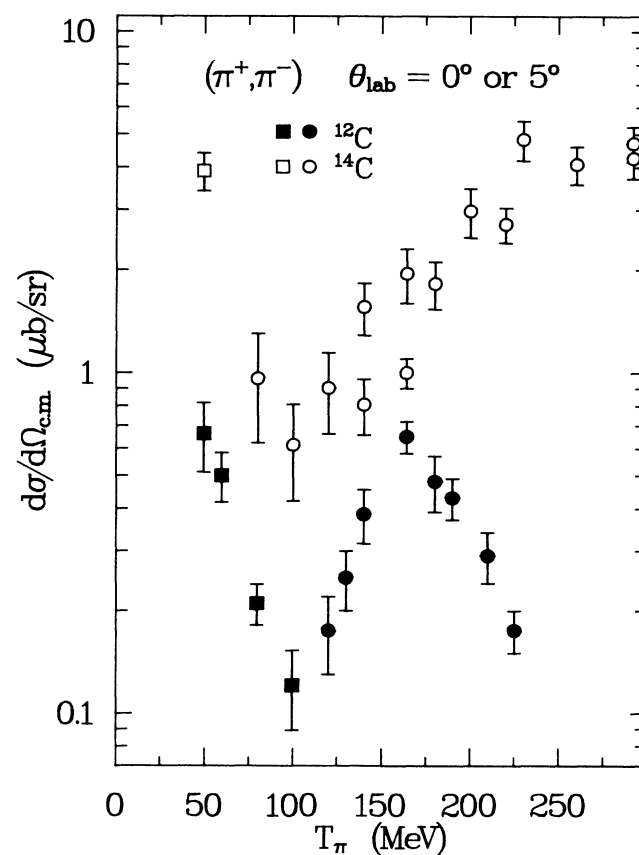


FIG. 4. Cross sections obtained by extrapolation to 0° from the present work (filled squares) compared with ^{12}C data at higher energies (filled circles, Ref. 2) and with other 0° or 5° data for ^{14}C (the open square is an extrapolation from Ref. 5 and the open circles are from Ref. 16).

- *Present address: Argonne National Laboratory, Argonne, IL 60439.
- ¹See, for example, Proceedings of the LAMPF Workshop on Pion Double Charge Exchange, Los Alamos National Laboratory Report LA-10550-C, 1985.
- ²L. C. Bland *et al.*, Phys. Lett. **128B**, 157 (1983).
- ³M. B. Johnson and E. R. Siciliano, Phys. Rev. C **27**, 1647 (1983); T. Karapiperis, M. Kobayashi, and M. Hirata, Phys. Lett. **144B**, 23 (1984); R. Gilman *et al.*, Phys. Rev. C **32**, 349 (1985).
- ⁴I. Navon *et al.*, Phys. Rev. Lett. **52**, 105 (1984).
- ⁵M. J. Leitch *et al.*, Phys. Rev. Lett. **54**, 1482 (1985).
- ⁶A. Altman *et al.*, Phys. Rev. Lett. **55**, 1273 (1985).
- ⁷Gerald A. Miller, Phys. Rev. Lett. **53**, 2008 (1984).
- ⁸T. Karapiperis and M. Kobayashi, Phys. Rev. Lett. **54**, 1230 (1985).
- ⁹W. R. Gibbs, W. B. Kaufmann, and P. B. Siegel, see Ref. 1, p. 90.
- ¹⁰B. Fick *et al.*, Phys. Rev. C **34**, 643 (1986).
- ¹¹L. G. Atencio *et al.*, Nucl. Instrum. Methods **187**, 381 (1981).
- ¹²B. Freedom *et al.*, Phys. Rev. C **23**, 1134 (1981); M. J. Leitch *et al.*, *ibid.* **29**, 561 (1984).
- ¹³G. Rowe, M. Salomon, and R. H. Landau, Phys. Rev. C **18**, 584 (1978).
- ¹⁴F. Ajzenberg-Selove, Nucl. Phys. **A433**, 1 (1985).
- ¹⁵R. Gilman *et al.*, Phys. Rev. C **29**, 2395 (1984).
- ¹⁶Peter A. Seidl *et al.*, Phys. Rev. C **30**, 973 (1984).
- ¹⁷R. Gilman *et al.*, Phys. Rev. C **33** 1082 (1986).
- ¹⁸Peter A. Seidl *et al.*, Phys. Lett. **154B**, 255 (1985).